Contents lists available at ScienceDirect

Asian Pacific Journal of Tropical Medicine

journal homepage:www.elsevier.com/locate/apjtm

Document heading doi:

Antiproliferative effect of silver nanoparticles synthesized using amla on Hep2 cell line

Fathima Stanley Rosarin[1], Vadivel Arulmozhi[1], Samuthira Nagarajan[2], Sankaran Mirunalini[1*]

[1]*Department of Biochemistry and Biotechnology, Annamalai University, Annamalai nagar-608 002, Tamilnadu, India*
[2]*Department of Chemistry, Annamalai University, Annamalai nagar-608 002, Tamilnadu, India*

ARTICLE INFO

Article history:
Received 24 May 2012
Received in revised form 31 July 2012
Accepted 5 September 2012
Available online 20 January 2013

Keywords:
Amla
AgNPs
Oxidative stress
Cytotoxicity
Antiproliferation

ABSTRACT

Objective: To synthesize silver nanoparticles by amla extract, screen the cytotoxic, oxidative stress and apoptotic effect of silver nanoparticles (AgNPs) on Hep2 cell line (laryngeal carcinoma cells) *in vitro*, and to compare the effect of *Phyllanthus emblica* (*P. emblica*) (amla) with AgNPs synthesized by amla and 5-FU. **Methods:** AgNPs was synthesized by *P. emblica* (aqueous extract) and nanoparticles were characterized UV-Vis spec, the presence of biomoloecules of amla capped in AgNPs was found by FT-IR analysis, shape and size were examined by SEM and DLS. Cytotoxicity of experimental drugs was tested to find IC_{50} value. ROS generation in cells have been measured by DCFH-DA staining, AO-EtBr, Rhodamine-123 staining and DNA fragmentation were performed to assess apoptotic cell death, mitochondrial membrane potential and apoptotic DNA damage, respectively. Oxidative stress was analyzed by measuring lipid peroxides and antioxidants level to understand the cancer cell death by pro-oxidant mechanism. **Results:** PE-AgNPs was synthesized and confirmed through kinetic behavior of NPs. The shape of PE-AgNPs was spherical and cubic since it was agglomerated, and the nanoparticle surface was complicated. Average particle size distribution of PE-AgNPs was found to be 188 nm. Potent biomolecules of *P. emblica* such as polyphenols were capped with AgNPs and reduced its toxicity. In cytotoxicity assay the concentration in which the maximum number of cell death was 60 μg/mL and 50 μg/mL for *P. emblica* (alone) and AgNPs, respectively and IC_{50} values were fixed as 30 μg/mL and 20 μg/mL. ROS generation, apoptotic morphological changes, mitochondrial depolarization, DNA damage and oxidative stress was observed as more in AgNPs treated cells than in *P. emblica* (30 μg/mL) (alone) treated cells and 5-FU treated cells gave similar result. **Conclusions:** The results suggest that the AgNPs are capped with biomolecules of amla enhanced cytotoxicity in laryngeal cancer cells through oxidative stress and apoptotic function on Hep2 cancer cells.

1. Introduction

Cancer is considered as one of the most deadly disease in the world with high mortality. Since there are many cancer therapies available, chemotherapy has become an integral component of cancer treatment for most cancers. In the area of oncology drug discovery, conventional chemotherapeutic agents still exhibit poor specificity in reaching tumor tissue and are often restricted by dose-limiting toxicity. The combination of developing controlled-release technology and targeted drug delivery may provide a more efficient and less harmful solution to overcome the limitations in conventional chemotherapy. Recent interest has been focused on developing nanoscale delivery vehicles, which are capable of controlling the release of chemotherapeutic agents directly inside cancer cells[1]. Nanomaterials are expected hopefully to revolutionize the cancer diagnosis and therapy. Nanoscale particles decorated with multiple functionalities are able to target and visualize tumor site via an imaging technology, thereby allowing for the early detection of cancer. Furthermore, intelligent nanosystems can be constructed as controlled delivery vehicles which are capable of delivering anticancer drugs to a predetermined site and then releasing them with a programmed rate, which can improve therapeutic efficacy[2].

In inorganic nanoparticles, metal nanoparticles have received considerable attention in recent years because of their unique properties and potential applications in

*Corresponding author: Dr. S. Mirunalini, assistant professor, Depatment of Biochemistry, Annamalai University, Annamalai nagar - 608 002,Tami nadu, India.
Tel: +91-(0)4144-239141
Fax: +91-(0)4144-238080

catalysis, photonics, optoelectronics, biological tagging and pharmaceutical applications. A number of approaches are available for the synthesis of silver nanoparticles (AgNPs). For example, silver ions are reduced by chemical, electrochemical, radiation, photochemical methods, Langmuir-Blodgett and biological techniques[3-9]. Among these methods, biological synthesis is a good way to fabricate benign nanostructure materials. Biological technique is less toxic and eco friendly, in the synthesis of nanoparticles capping agents are used. Capping agent is absorbed by nanoparticles. They are usually organic molecules, and used to aid stabilization of nanoparticles. Silver nanoparticles were synthesized by various plant materials as capping agents such as papaya[10] and neem[11]. Polyphenols of *Phyllanthus emblica* (*P. emblica*) includes hydrolysable tannins, flavonoids, alkaloids, gallic acid, ellagic acid and quercetin[12], and this plant exhibits antioxidant[13], adaptogenic[14], and hepato-protective action[15]. Due to the existence of the conjugated ring structures and hydroxyl groups, many phenolic compounds have the potential to function as antioxidants by scavenging superoxide anion[16] and singlet oxygen[17]. Metal nanoparticles can be synthesized in the average size of more than 50 nm, therefore their large surface area has the ability to carry a relatively high drug dose. Functionalizing the surface of conventional metallic nanoparticles like gold and silver to carry drugs is under investigation.

In the present study, we have made an attempt to investigate the anticancer effect of PE-AgNPs and drug delivery efficacy of Ag nanoparticles on Hep2 (laryngeal epidermoid carcinoma, a common malignant tumor of head and neck)[18] cell line which has not been previously studied. The biological applications of silver nanoparticles (AgNPs), antimicrobial properties in particular have been widely studied[19]. AgNPs are known to be cytotoxic to both normal and cancer cells in mammals[20] and the modes of interactions of AgNPs have been investigated in different prokaryotic and eukaryotic systems[21-23]. Since nanoparticles (NPs) are more biocompatible than the conventional therapeutics, they are exploited for drug encapsulation and delivery[24]. It has been stressed over the years that size reduction of NPs play an important role in improving their bioavailability as well as compatibility for therapeutical applications in diseases like cancer[25]. Silver nanoparticles (AgNPs) have a great potential in cancer management because it selectively involved in disruption of the mitochondrial respiratory chain by AgNPs leading to production of ROS and interruption of ATP synthesis, which in turn cause DNA damage[26,21]. Based on the conflicting results, here is an urgency to evaluate cytotoxicity and apoptotic properties of PE-AgNPs on hep2 cells. In order to study the properties of PE-AgNPs to induce apoptosis in cancer cells, it was compared with a standard reference drug 5-flourouracil (5-FU) and we also compared *P. emblica* fruit extract (alone) with its encapsulated AgNPs. For this study, we employed a well characterized AgNPs to access its apoptotic function via its cytotoxicty and oxidative stress. Dose was fixed and applied in the Hep2 cells by the cytotoxicity test. Based on this study and our ability to access the interaction and interference with a wide range of biological functions, PE-AgNPs employed in the present study provide a unique opportunity to investigate oxidative stress, intracellular ROS generation, apoptotic bodies and apoptotic DNA fragmentation, and mitochondrial membrane potential and toxicity in human laryngeal carcinoma cells (Hep2 cell line). Though the AgNPs induces mitochondrial mediated apoptosis[27], we have made an attempt to cap the AgNPs with potent biomolecules of *P. emblica* and we assessed the toxicity and examined the apoptotic function of PE-Ag NPs which comprised of biomolecules of *P. emblica* and silver precursors.

2. Materials and methods

2.1. Silver nanoparticles

The silver nanoparticles were synthesized using previously published procedure in which AgNPs were produced through ion reduction and subsequent stabilization using aqueous extract of *P. emblica* fruits. In this method *P. emblica* pericorps were initially rinsed thrice in distilled water and dried on paper toweling. About 25 g of fruit were cut into fine pieces and boiled with 100 mL sterile distilled water for 5 minutes and filtered through Whatman No.1 filter paper twice. The filtrate was stored at 4 ℃ and used for the present study. About 10 mL of aqueous fruit extract was added into the 100 mL aqueous solution of 1 mM $AgNO_3$ (AR)[28]. The 100 mL of 1 mM silver nitrate solution was reduced using 10 mL of *P. emblica* extract at room temperature within 10 min. Ag^+ ion reduction was monitored by measuring the UV-vis spectrum of the reaction medium at various time intervals (5 min to 78 h) in room temperature. The pellet of AgNPs obtained after centrifugation was air dried and mixed with KBr and the KBr-AgNPs pellet was subjected to FT-IR to ensure the formation of silver nanoparticles with encapsulation of biomolecules of *P. emblica*. A scanning electron microscope was used to record the micrograph images of synthesized AgNPs, the particle size distribution of AgNPs was evaluated using dynamic light scattering measurements. These well characterized silver nanoparticles were further used for cytotoxicity and oxidative stress on cancer cells.

2.2. Cell culture

The human laryngeal carcinoma cell line (Hep2) was purchased from National Centre for Cell Science, Pune, India. The cells were cultured as monolayer in MEM supplemented with 10% FBS, 1% glutamine and 100 U/mL penicillin-streptomycin at 37 ℃ in 5% CO_2 atmosphere, stocks were maintained in 25 cm^2 tissue culture flasks. A stock solution of PE (1 mg/mL) and PE-AgNPs (1 mg/mL) was prepared in 0.5% dimethyl sulphoxide (DMSO) (w/v) and stored at 4 ℃ further dilution was made in culture media to obtain the desired concentrations. The final concentrations of DMSO in the culture medium were not more than 0.01% (v/v). 0.01% DMSO was used as a sham control.

2. 3. Cytotoxicity assay

Cells were treated with different concentration of PE and PE-AgNPs (1, 5, 10, 20, 30, 40, 50 μg/mL) and the cytotoxicity was observed by (3-4, 5-dimethyl thiazol-2yl)-2, 5-di phenyl tetrazolium bromide (MTT) assay. MTT assay was first proposed by mossmon[29]. IC_{50} value was calculated and optimum dose of PE and PE-AgNPs was fixed in this assay for further study. It is a colorimetric assay for measuring the activity of enzymes that reduce MTT to purple color. Formazan product is directly proportional to viable cells. 10 μL of MTT solution (5 mg/mL in PBS) was added to each culture well after 24 hours of incubation with PE and PE-AgNPs treatment. The color was allowed to develop for additional 4 hours incubation. An equal volume of DMSO was added to stop the reaction and to solubilize the blue crystals. The absorbance was taken using UV-visible spectrophotometer (Elico SL159, India) at a wavelength of 570 nm. OD value was subjected to sort-out percentage of viability by using the following formula, OD value of experimental samples.

$$\text{Percentage of cell viability} = \frac{\text{OD value of experimental sample (AgNPs)}}{\text{OD value of experimental control (untreated)}} \times 100$$

2. 4. Cell treatment

The Hep2 cells were treated with PE and PE-AgNPs in the following concentrations as revealed by MTT assay. They are Group Ⅰ - Control (untreated cancer cells), Group Ⅱ - Hep2 cells (30 μg/mL PE), Group Ⅲ - Hep2 cells + 20 μg/mL PE-AgNPs and Group Ⅳ - Hep2 cells + 30 μg/mL 5-FU. After treatment they were incubated at 37 ℃ in 5% CO_2 incubator after 24 h incubation. The cells were harvested by trypsinization for further experiments.

2. 5. Reactive oxygen species generation

Reactive oxygen species was assessed following the procedure described by Jesudason *et al*[30]. Cells were seeded in 96 well plate and incubated with PE extract (30 μg/mL), PE-AgNPs (20 μg/mL) and 5-FU (30 μg/mL for 24 h. After incubation, fluorescent dye 2′, 7′-dichlorfluorescein-diacetate (DCFH-DA) a non-fluorescent probe that can penetrate into the intracellular matrix of cells, was added to the cells. It was oxidized by ROS to fluorescent dichlorofluorescein (DCF) which were then kept in incubator for 30 min. Then the cells were washed with PBS to remove the excess dye.

2. 6. Mitochondrial membrane potential

Mitochondrial membrane potential was evaluated following the procedure described by Bhosle *et al*[31] using the Rhodamine-123 (Rh-123) which is a lipophilic cationic dye, highly specific for mitochondria. The cells were seeded in 96 well plate and treated with PE (30 μg/mL), PE-AgNPs (20 μg/mL) and 5-FU (30 μg/mL) and incubated for 24 h. After incubation of the cells, fluorescent dye Rh-123 (5 mmol/L) was added to the cells and kept in incubator for 30 min. Then the cells were washed with PBS and viewed under fluorescent microscope using blue filter.

2.7. Apoptotic morphological changes

The apoptotic bodies which were the result of treatment with PE-Ag NPs was assessed by the method of Lakshmi *et al*[32]. Apoptotic nuclei exhibits typical changes such as nuclear condensation and fragmentation were stained by AO/EtBr to know the dead apoptotic cells. Cells were treated with PE (30 μg/mL), PE-AgNPs (20 μg/mL) and 5-FU (30 μg/mL), and incubated in CO_2 incubator for 24 h. The cells were fixed in methanol: glacial acetic acid (3:1) for 30 min at 37 ℃. The cells were washed with PBS and stained in 1:1 ratio of AO/EtBr, stained cells were immediately washed and viewed under a fluorescent microscope with a magnification of 40×.

2. 8. Apoptotic DNA fragmentation

Apoptotic DNA fragmentation is a key feature of programmed cell death and also occurs in certain stages of necrosis. DNA damage was estimated by agarose gel electrophoresis of DNA fragmentation[33]. Hep2 cells were treated with PE (30 μg/mL), PE-AgNPs (20 μg/mL) and 5-FU (30 μg/mL). Treated and untreated cells were collected by centrifugation at 3 000 rpm for 15 min at 4 ℃. The cell pellet was suspended in cell lysis buffer (Tris Hcl 10 mmol/L pH 7.4, Triton-×100, 0.5%) and kept at 4 ℃ for 10 min. The lysate was centrifuged at 25 000 rpm for 20 minutes. The supernatant was incubated with RNAase of 40 μg/L at 37 ℃ for 1 h then incubated with proteinase K 40 μg/L at 37 ℃ for 1 h. To the final aqueous phase 40 μL of 3.5 M ammonium acetate was added, to this ice cold isopropanol was added and centrifuged at 25 000 rpm for 15 min and dried. After drying, DNA was dissolved in TE buffer and separated by 2% agarose gel electrophoresis at 100 V for 50 min and the DNA Damage was analyzed by gel documentation (alpha innotech image analyzer).

2. 9. Lipid peroxidation

Accumulation of lipid peroxides in the cell is associated cellular stress which leads to cancer cell death. The cells were harvested by trypsinization, the cell pellet obtained was suspended in PBS. The suspension was taken for biochemical estimations. The level of lipid peroxidation was determined by analyzing TBA-reactive substances (TBARS)[34]. The pink chromogen formed by the reaction of 2-TBA with breakdown products of lipid peroxidation was

measured.

2. 10. Antioxidants

Superoxide dismutase (SOD) activity was assayed[35] based on the inhibition of the formation of reduced nicotinamide adenine dinucleotidephenazine methosulphate-NBT complex. Catalase (CAT) activity was assayed[36] by quantifying the hydrogen peroxide after reacting with dichromate in acetic acid. The activity of glutathione peroxidase (GPx) was assayed by a known amount of enzyme preparation was allowed to react with hydrogen peroxide and reduced glutathione (GSH) for a specified period[37]. Then, the GSH content remaining after the reaction was measured. The total GSH content was measured based on the development of a yellow color when 5′5-dithiobis-2-nitrobenzoic acid was added to compound containing sulphydryl groups[38].

2.11. Statistical analysis

The statistical analysis was done among the experimental groups with control and normal groups using SPSS software Version 16 (SPSS Inc., Chicago, IL, USA). The One-way ANOVA was done for expressing experimental significance of the present study. Statistical significance was accepted at a level of $P < 0.05$.

3. Results

3.1. Nanoparticle synthesis and characterization

When aqueous extract of *P. emblica* was added to silver nitrate solution and stirred for 1 h, the resultant solution was brownish orange (Figure 1). The change in colour (brownish orange) is due to excitation of the surface plasmon vibration of the metal nanoparticles. The SPR bands of silver colloid for different intervals were appeared at 428 to 438 nm and the λ_{max} is red shifted from 428 to 438 nm (Figure 2). Subsequently, the particles were capped with polyphenols present in the *P. emblica*, these biomolecules stabilized nanoparticles and capping of potent biomolecules was confirmed by FTIR. FT-IR analysis revealed the strong bands at 3 387, 1 725, 1 619, and 1 058 cm^{-1}. Similarly band at 3 387 cm^{-1} due to functional group in alcohols and phenolic compounds shifted to 3 425 cm^{-1} for silver nanoparticles. For bands 1 725 cm^{-1} and 1 619 cm^{-1} in the curve shifted to 1 747 cm^{-1}. The band at 1 725 cm^{-1} band shifted to 1 747 cm^{-1} (carbonyl groups) and the weaker band at 1 249 cm^{-1} shifted to 1 316 cm^{-1} (C-O Stretching). The band at 1 058 cm^{-1} was shifted to 1 020 cm^{-1} (C-O-C and C-OH vibrations of the protein). In FT-IR spectra the band shifted at 1 725, 1 619, and 1 058 cm^{-1} (Figure 3). In this project, we utilized PE-AgNPs with spherical and cubic shapes with little agglomeration and average particle size distribution with 188 nm (Figure 4 and 5). The approach employed in the production of these materials (PE-AgNPs) is low cost and ecofriendly. Moreover this method confirms the well characterized AgNPs which carries drug and exhibits its activity on any counterparts.

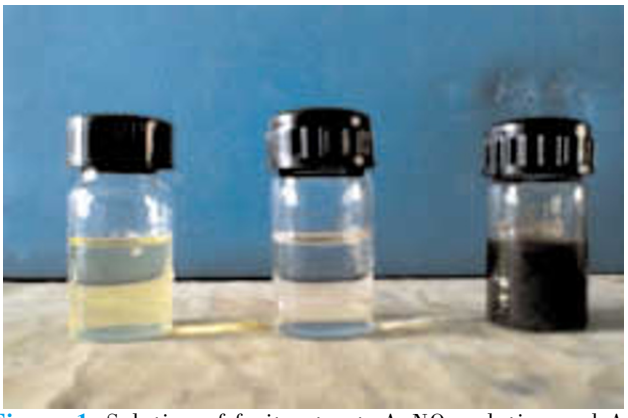

Figure 1. Solution of fruit extract, $AgNO_3$ solution and Ag nanoparticles (From left to right).

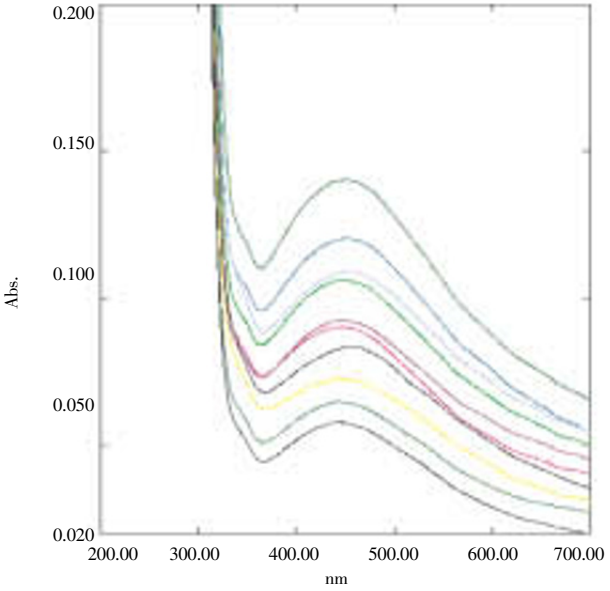

Figure 2. UV-Vis spectra of the Ag nanoparticles prepared with 1mM aqueous $AgNO_3$ solution with 10% *P. emblica* extract, spectra of nanoparticle solution was taken at different intervals from 5 minutes to 78 hours.

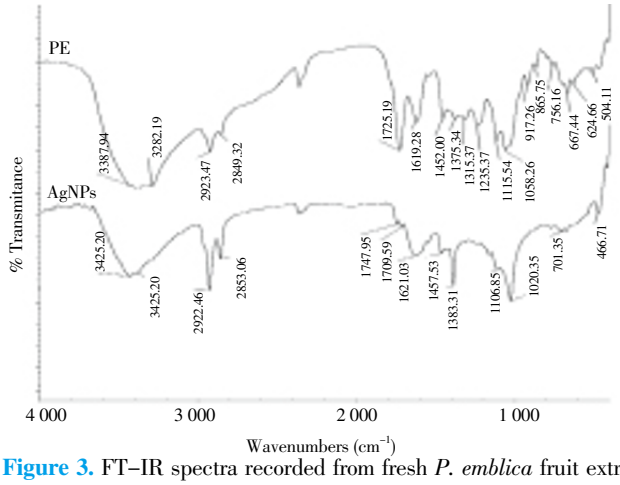

Figure 3. FT-IR spectra recorded from fresh *P. emblica* fruit extract

dried powder and FT-IR spectra recorded from extract-reduced silver nanoparticles (AgNPs).

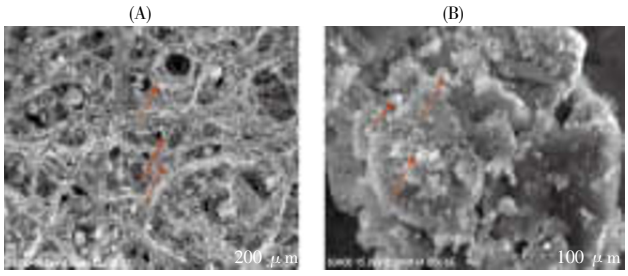

Figure 4. SEM images of silver nanoparticles from *P. emblica* at 15.0 kV 5.6 mm × 2.00 k and 20 μm (A) same image at 15.0 kV 5.5 mm × 4.00 k and 10 μm (B). Arrow marks indicates the nanoparticles.

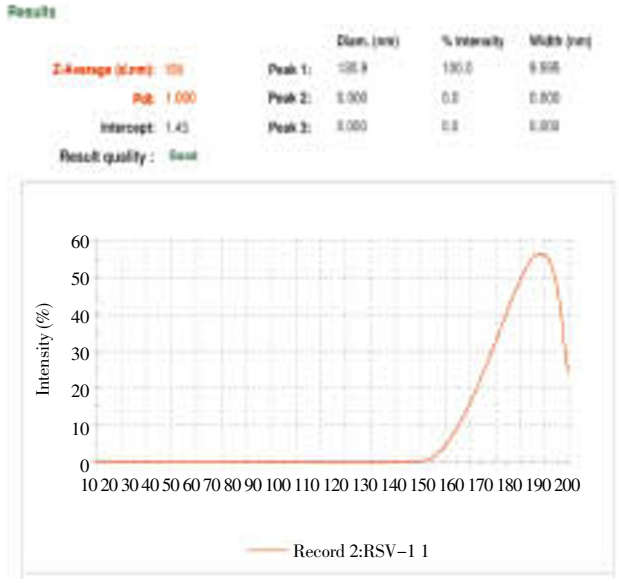

Figure 5. Formation of Ag nanoparticles synthesized with amla by ion reduction method monitored by DLS particle size distribution of AgNPs.

3.2. Effect of PE and PE-AgNPs on cell proliferation

Effect of AgNPs on cell proliferation was determined by MTT assay. The proliferation of Hep2 cells was significantly inhibited by AgNPs. The inhibitory effect was observed after 24 h incubation. Figure 6 shows the changes in the percentage of cell viability in control, *P. emblica* (PE) and PE-AgNPs treated (5, 10, 20, 30, 40, 50 and 60 μg/mL) in Hep2 cells. There was a 100% cell death at 60 μg/mL concentration of PE. Conversely, PE-AgNPs showed 100% cell death at 40 μg/mL concentration in Hep2 cells. Hence, the inhibitory concentration 50 (IC_{50}) was fixed as 30 μg/mL for PE and 20 μg/mL for PE-AgNPs in Hep2 cells. This IC_{50} value was used for following experiments. In this study, we compared the anticancer potential of PE-AgNPs with the standard anticancer drug 5-Fluoro Uracil (30 μg/mL).

3.3. PE-AgNPs generates intracellular ROS

Level of ROS was observed by green fluorescence in control, PE and PE-Ag NPs treated cells were depicted in Figure 7. PE (alone) treatment increased ROS level in Hep2 cells. PE-AgNPs treatment (20 μg/mL) significantly increased ROS level in Hep2 cells. We observed 5-Fluorouracil (30 μg/mL) treatment showed the same result in Hep2 cells (Figure 7).

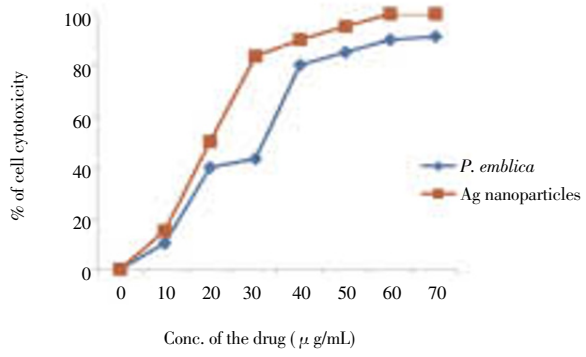

Figure 6. Cytotoxicity assay.

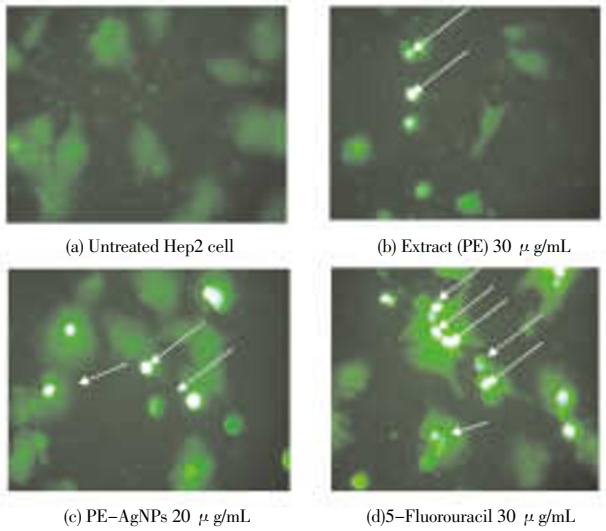

Figure 7. Intracellular ROS generation: Fluorescence microscopic images of intracellular ROS measurement by DCFH-DA staining. Arrow mark (→) represents DCF fluorescence in 30 μg/mL P.E treatment (b). DCF fluorescence is on increase in 20 μg/mL of PE-AgNPs treated cells (c). This result was compared with positive control treatment (d).

3.4. P.E-AgNPs alters mitochondrial membrane potential ($\Delta\Psi_m$)

Depolarized mitochondria membrane was found by the ability of cells to receive dye, Changes in mitochondrial membrane potential in control, PE and PE-AgNPs-treated cells were depicted in Figure 8. PE-AgNPs treatment at the concentration of 20 μg/mL significantly increased mitochondrial depolarization in Hep2 cells. PE-AgNPs treated cells underwent more mitochondrial depolarization (Figure 8c) than PE (30 μg/mL) treated cells (Figure 8b). PE-AgNPs showed high level of mitochondrial depolarization Hep2 cells. We observed similar result with positive control 5-fluorouracil (30 μg/mL) (Figure 8d).

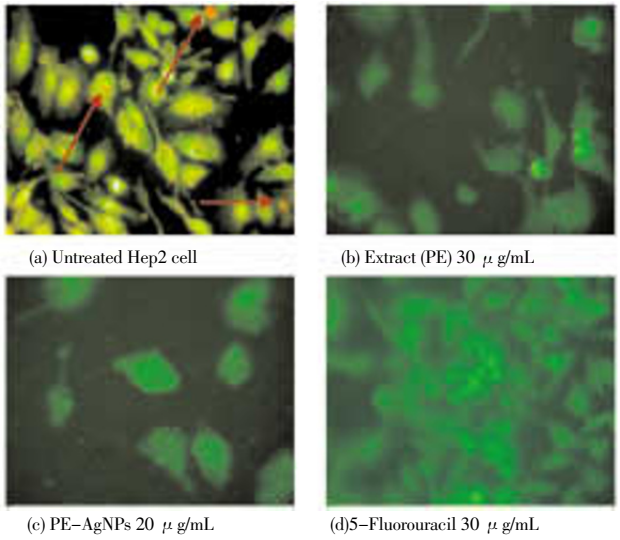

Figure 8. Mitochondrial membrane potential: Fluorescence microscopic images of mitochondrial membrane potential by Rh-123 staining.
An Arrow mark (→) represents dye accumulation in control group (a). An Arrow mark (→) represents no dye accumulation in 30 μg/mL PE treatment group (b). There is no accumulation of Rh-123 in 20 μg/mL PE-AgNPs treatment group (c). This result was compared with the cells treated with positive control (d).

3.5. Effect of PE-AgNPs on apoptotic morphological changes

Figure 3 shows the effect of control, PE and PE-AgNPs on apoptotic morphological changes by orange emission in Hep2 cells for apoptotic cell death. Figure 9 show that the nuclear morphological changes in PE-AgNPs (20 μg/mL) treated cells. PE-AgNPs treated cells underwent more apoptotic morphological changes than PE (30 μg/mL) treated cells. We observed similar result with positive control 5-fluorouracil (30 μg/mL).

3.6. AgNPs induces apoptosis by DNA damage

DNA fragmentation of Hep2 cells were depicted by its DNA ladder in Figure 10. PE treatment at the concentration of 30 μg/mL significantly increased DNA fragmentation in Hep2 cells. PE-AgNPs treated cells underwent more DNA fragmentation than cells treated with PE at the concentration of 30 μg/mL. We observed similar result with positive control 5-fluorouracil (30 μg/mL) (Figure 10).

3.7. Changes in the levels of lipid peroxidation and antioxidants status

We measured lipid peroxidation indices (TBARS) in Hep_2 cell line. PE-AgNPs (20 μg/mL) treatment increased the levels of TBARS when compared to PE (30 μg/mL) treated cells (Figure 11). Figure 12 shows the activities of enzymatic antioxidant such as SOD, CAT and GPx in untreated cells, PE-AgNPs and PE in Hep2 cells. PE-AgNPs (20 μg/mL) treatment decreased the activities of enzymatic antioxidants in Hep2 cells when compared to PE (30 μg/mL). We observed similar result with positive control 5-fluorouracil (30 μg/mL). GSH is the important cellular antioxidant (Figure 12). It shows that P.E-AgNPs (20 μg/mL) treatment decreased the levels of GSH in Hep2 cells. PE-AgNPs enhanced in reducing the levels of GSH in Hep2 cells than PE (30 μg/mL). We observed similar result with positive control 5-fluorouracil (30 μg/mL).

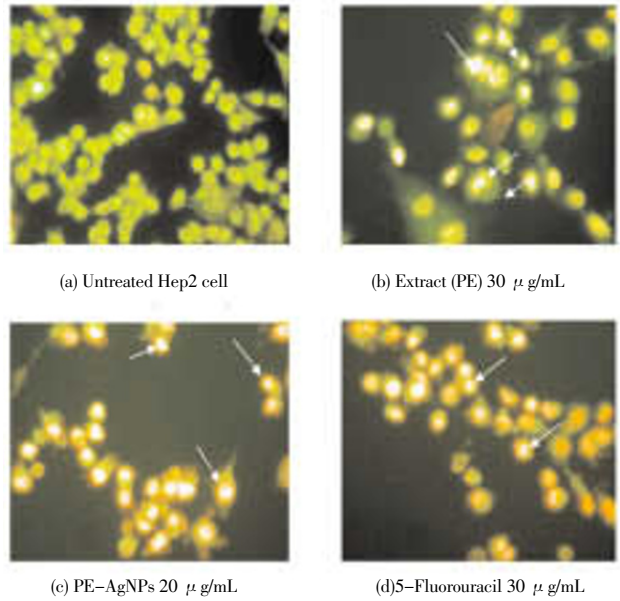

Figure 9. Apoptotic morphological changes by dual staining: Fluorescence microscopic images of apoptotic morphology by dual staining.
Arrow mark (→) represents orange-colored cells which are late apoptotic cells. Orange colored cells are present in PE treated cells (b). Number of orange colored cells is on increase in PE-AgNPs treated cells (c). This result was compared with cells treated with positive control (d).

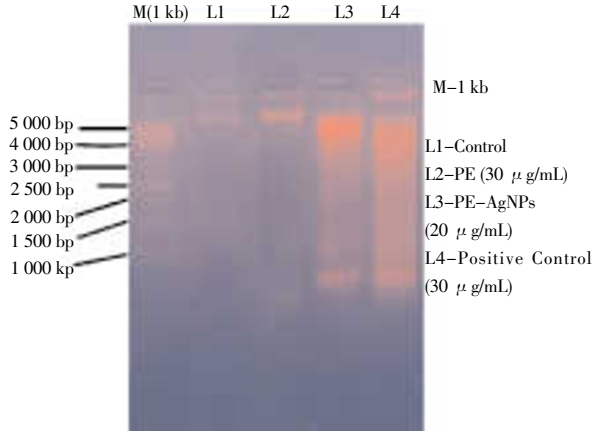

Figure 10. DNA fragmentation.
M is 1kb DNA used as a marker DNA, lane1 (L1) is DNA of control cells showing clear bands indicates no apoptosis. Lane 2 (L2) is DNA of *P. emblica* treated cells showing small DNA ladder indicating apoptosis by DNA damage begins. Lane 3 (L3) is DNA of PE-AgNPs treated cells showing a large DNA ladder indicates more apoptosis compared to PE treated cells. This is compared with Lane 4 (L4) DNA of positive control treated cells.

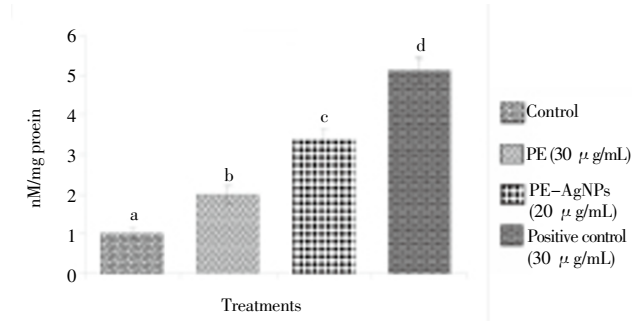

Figure 11. TBARS level.

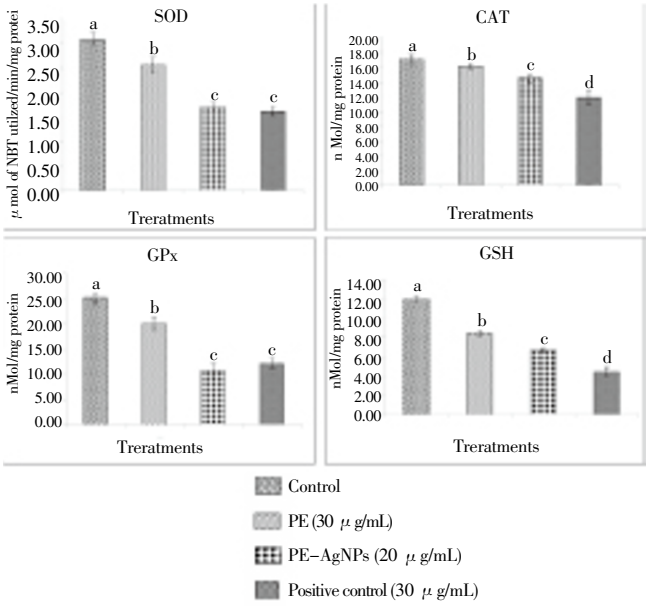

Figure 12. Antioxidant level.

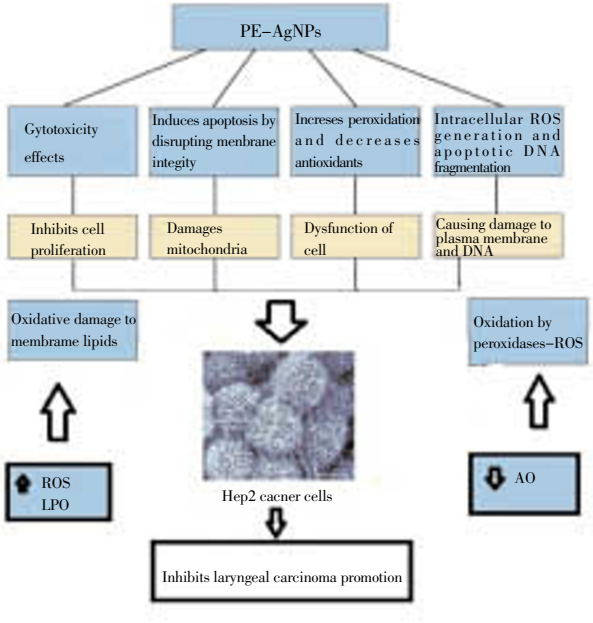

Figure 13. Possible mechanism for antiproliferative effect of silver nanoparticles in cancer therapy.

4. Discussion

The Ag NPs used in this study were synthesized by green synthesis method in which AgNPs were produced through chemical reduction and subsequent stabilization using aqueous extract of amla, these AgNPs were found to be very stable. When aqueous extract of amla was added to silver nitrate solution and stirred for 1 h, the resultant solution was brownish orange[39]. The change in colour (brownish orange) is due to excitation of the surface plasmon vibration of the metal nanoparticles. The SPR bands of silver colloid for different intervals were appeared at 428 to 438 nm and the λ_{max} is red shifted from 428 to 438 nm. Subsequently, the particles were capped with polyphenols present in the amla, these biomolecules stabilize nanoparticles. In this study we found spherical and cubic shapes and nanoparticle surface is complicated due to agglomeration and average particle size distribution with 188 nm. The approach employed in the production of these materials (PE-AgNPs) is low cost and ecofriendly. Moreover this method confirms the characterized AgNPs which carries drug and exhibits its activity on any counterparts.

Evaluation of cytotoxicity in laryngeal Hep2 cells by PE-AgNPs was performed using MTT assay (viability assay). Hep2 cell line was previously used for various anticancer studies[40]. Decreased mitochondrial function was found in cells which are exposed to PE-AgNPs (5-60 μg/mL) in a dose-dependent manner as seen in the MTT assay. We observed AgNPs treatment (24 hours incubation) significantly decreased percentage of cell viability in Hep2 cells. This result is analogous to the one reported by Hussain *et al*[20] where cytotoxicity due to decreased mitochondrial function was indicated in a rat liver derived cell line (BRL 3A) exposed to silver nanoparticles at concentrations in the range of 5-50 μg/mL. Moreover, previous reports show that AgNPs induce oxidative cell damage in human liver cells through inhibition of mitochondria-involved apoptosis[41] Cells underwent concentration dependent cytotoxicty by AgNPs, and a significant decrease in the cell viability was observed as inhibitory concentration (IC_{50} value). These concentrations were further used for all experiments; they are 30 μg/mL and 20 μg/mL for PE and PE-AgNPs respectively. The mechanism of cytotoxicity by apoptosis was further evaluated.

Nanoparticles have been shown to generate the formation of reactive oxygen species (ROS), therefore, ROS formation was assessed to determine pro-oxidant effect of PE-AgNPs on cancer cells in order to kill them. In the present study, a fluorogenic assay was used to measure the production of ROS at 24 h culture setup. It is now well established that the generation or external addition of ROS can cause cell death by two distinct pathways, *viz.* apoptosis or necrosis. ROS are known to trigger the apoptotic cascade, via caspases, which are considered as the executioners of apoptosis[42].

Many studies have implicated intracellular ROS in the signal transduction pathways leading to apoptosis[43,44]. Recently, it was reported that apoptosis induced by exposure to AgNPs was mediated by oxidative stress in fibroblast, muscle and colon cells[45,46]. we observed ROS generation during PE-AgNPs (20 μg/mL) treatment the doses which caused significant increase in ROS correlated with the doses that significantly affected cell viability decreased in the MTT assay. These data suggest that PE-AgNPs can induce cell death in Hep2 cells through a ROS-mediated apoptotic process as suggested in the pro-oxidant effect in Hep2 cells. Our results show that PE-AgNPs trigger apoptosis via ROS generation in *in vitro* systems. However, the function of ROS in PE-AgNPs induced liver cells death is currently unclear.

Production of ROS disrupts the mitochondrial membrane permeability (MMP) so we tended to assess the effect of AgNPs on disrupting MMP[46]. PE-AgNPs treatment at the concentration of 20 μg/mL significantly increased mitochondrial membrane depolarization in Hep2 cells. To explore the possible molecular mechanisms of PE-AgNPs-mediated cell death, we measured deviations in the levels of regulators involved in apoptosis. Mitochondria are important signaling centers during apoptosis, and the loss of mitochondrial integrity can be induced or inhibited by many regulators of apoptosis[46,47]. In many cases, oxidative stress induces caspase activation through cytochrome c release from the mitochondrial inter-membrane space into the cytosol[46,48]. In our study, PE-AgNPs induced mitochondrial release of cytochrome c and the loss of $\Delta\Psi_m$ is a result of induced cell death. Cytochrome c release initiates a cascade that leads to the activation of caspase 3 through Apaf-1 and caspase 9[49,50]. Our results also demonstrated that cytochrome c was exempted from mitochondria into the cytoplasm, followed shows accumulation of Rh-123 dye in the control group and the Rh-123 accumulation were decreased in PE-AgNPs treated cells as the membrane potential decreased. Hsin *et al*[45] have reported that mitochondria are a major site for PE-AgNPs-induced ROS generation. This suggests that PE-AgNPs activates the intrinsic apoptotic pathway, which is characterized by disruption of $\Delta\Psi_m$, and cytochrome c release from the mitochondria. Since there appeared to be a differential mechanism of cell death being further studies explored the changes membrane blebbing and chromatin condensation related to apoptotic DNA damage. The apoptosis can be assessed by measuring the apoptotic bodies or cell fragments. To explore the method of cell death in Hep2 cells by PE-AgNPs, we observed apoptotic morphological changes by AO/EtBr staining. The morphological observation showed typical apoptotic indices in different treatment groups. The increased ROS levels and subsequent loss of mitochondria membrane potential might be the cause for the increased apoptotic morphological changes in the PE-AgNPs treated cells. However, late apoptotic cells can be falsely detected as necrotic cells due to membrane damage. Accordingly, cells testing positive of apoptosis at an early time point could be detected as necrotic cells after longer exposures[51-54]. The result shows that the nuclear morphological changes in PE-AgNPs (20 μg/mL) treated cells. PE-AgNPs treated cells underwent more apoptotic morphological changes than PE (30 μg/mL) treated cells. We observed similar result with positive control 5-Fluorouracil (30 μg/mL). Apoptosis has previously been found to occur in response to treatment with other nanomaterials such as TiO_2[55] and nanoscale hydroxyapatite[56].

DNA fragmentation of Hep2 cells were depicted. The role of apoptosis in PE-AgNPs toxicity was evaluated by DNA fragmentation, the presence of oligonucleosomal DNA fragments or DNA laddering at treatment of PE-AgNPs concentration around 20 μg/mL indicates apoptotic cell death. Cytotoxicity (necrosis) at higher doses of PE-AgNPs (40 μg/mL) is clearly demonstrated by total lack of caspase-3 activity. This PE-AgNPs concentration matches well with the observed IC_{50} values and hence supports the findings of apoptotic morphological changes assay. Further, our data clearly show that at concentrations up to 20 μg/mL (PE-AgNPs) results cell death occurs due to DNA damage alone. Cleavage of chromosomal DNA into oligonucleosomal size fragments is an integral part of apoptosis. Elegant biochemical work identified the DNA fragmentation factor as a major apoptotic endonuclease for DNA fragmentation *in vitro*.

Our study unveiled cytotoxicity was induced by PE-AgNPs through oxidative stress. It is noteworthy that the adverse effects of nanoparticles were also concentration dependent. In the case of nanoparticle agglomeration and subsequent precipitation, uptake rate of nanoparticles will drop, which could be observed as a decrease in ATP depletion and cytotoxicity. When PE alone was used, it showed less cytotoxicity than PE-AgNPs through oxidative mechanism in Hep2 cells. This observation ensures biocompatibility of *P. emblica* as capping agent in nanoparticles. The cell viability in all the groups was comparable to that of control. To investigate the potential role of oxidative stress as a mechanism of PE-AgNPs induced toxicity, we measured lipid peroxidation (TBARS) and antioxidants such as SOD, CAT, GPx and GSH in Hep2 cell line. Our results show significant increase in lipid peroxidation and decreased GSH levels in PE-AgNPs-treated Hep2 cells. Previous studies on rat liver derived cell line (BRL 3A) by Hussain *et al*[20] showed that there was a significant increase in ROS and decrease in GSH levels at 25 and 50 μg/mL of AgNPs. A significant elevation of lipid peroxidation and marginal GSH depletion was demonstrated in a fish model upon exposure to fullerenes[57]. These results also propose oxidative damage to cells after exposure to AgNPs. Conversely, we observed decreased activities of antioxidant enzymes, *i.e.*, SOD, CAT, and GPx in PE-AgNPs-treated Hep2 cancer cells. Similar

observations were made by Tirkey *et al*[58] decreased the activity of SOD, CAT and GPx due to carbon tetrachloride induced oxidative stress in rat liver and kidney cells. PE as a capping agent also plays a major role in oxidative stress in Hep2 cells, it also has polyphenols such as terpenoids and triterpenoids which act as antiproliferative agents and they also has many therapeutic values. A recent review paper on *P. emblica* has been described to possess anticancer, antihyperlipidemic and hepatoprotective activities[59]. This friut has compounds such as vitamin C, ellagic acid and gallic acid. The apoptotic activity was enhanced when they are capped with AgNPs and it reduces the toxicity of AgNPs. This combined effect was assesed in this study.

Polyphenols and proteins present in *P. emblica* fruit are encapsulated with AgNPs and gives stability. These nanoparticles were compared with anticancer drug 5-FU to understand the cytotoxic effect on cancer cells. The cytotoxicty can be possibly controlled cell death because we found the prooxidant mechanism in our results. By studying gene expression (pro apoptotic gene) one can confirm the apoptotic function of the PE-Ag NPs. The results summarize that PE-AgNPs initiates the cancer cell death by lessening cell proliferation, antioxidant status, increasing intracellular ROS, alteration in mitochondrial membrane potential, lipid peroxidation, DNA fragmentation and apoptosis in Hep2 laryngeal carcinoma cell line. Therefore, in the present study we have highlighted the correlations among cytotoxicity, oxidative stress and apoptotic potential of amla-silver nanoparticles. When compounds have anticancerous activity are capped with AgNPs, it enhance its apoptotic property. Since AgNPs are used in an increasing number of applications, further studies on the mechanisms of AgNPs uptake and cytotoxicity are required to rate the risks and benefits of nano-silver.

Conflict of interest statement

We declare that we have no conflict of interest.

References

[1] Gu FX, Karnik R, Wang AZ, Alexis F, Levy-Nissenbaum E, Hong S, et al. Targeted nanoparticles for cancer therapy. *Nanotoday* 2002; **2**: 14-21.

[2] Mirkin CA, Nel A, Thaxton CS. Applications: Nanobiosystems, medicine, and health. *Sci Policy Reports* 2011; **1**: 305-374.

[3] Sun Y, Yin Y, Mayers BT, Herricks T, Xia Y. Uniform silver nanowires synthesis by reducing $AgNO_3$ with ethylene glycol in the presence of seeds and poly (vinyl pyrrolidone). *Chem Mater* 2002; **14**: 4736-4745.

[4] Yin B, Ma H, Wang S, Chen S. Electrochemical synthesis of silver nanoparticles under protection of poly (*n*-vinylpyrrolidone). *J Phys Chem B* 2003; **107**: 8898-8904.

[5] Dimitrijevic NM, Bartels DM, Jonah CD, Takahashi K, Rajh T. Radiolytically induced formation and optical absorption spectra of colloidal silver nanoparticles in supercritical ethane. *J Phys Chem B* 2001; **105**: 954-959.

[6] Callegari A, Tonti D, Chergui M, Photochemically grown silver nanoparticles with wavelength-controlled size and shape. *Nano Lett* 2003; **3**: 1565-1568.

[7] Zhang L, Shen YH, Xie AJ, Li SK, Wang C. One-step synthesis of silver nanoparticles in self-assembled multilayered films based on a Keggin structure compound. *J Mater Chem* 2008; **18**: 1196-1203.

[8] Swami A, Selvakannan PR, Pasricha R, Sastry M. One-step synthesis of ordered two-dimensional assemblies of silver nanoparticles by the spontaneous reduction of silver ions by pentadecylphenol langmuir monolayers. *J Phys Chem B* 2004; **108**: 19269-19275.

[9] Naik RR, Stringer SJ, Agarwal G, Jones S, Stone MO. Peptide templates for nanoparticle synthesis derived from polymerase chain reaction-driven phage display. *Adv Funct Mater* 2002; **14**: 25-30.

[10] Jain D, Daima HK, Kachhwaha S, Kothari SL. Synthesis of plant-mediated silver nanoparticles using papaya fruit extract and evaluation of their anti microbial activities. *Dig J Nanomat Biostruc* 2009; **4**: 557-563.

[11] Shankar S, Rai A, Ahmad A, Sastry M. Rapid synthesis of Au, Ag, and bimetallic Au core-Ag shell nanoparticles using Neem (*Azadirachta indica*) leaf broth. *J Coll Inter Sci* 2004; **275**: 496-502.

[12] Anila L, Vijayalakshmi NR. Flavonoids from *Emblica officinalis* and *Mangifera indica*-effectiveness for dyslipidemia, *J Ethnopharmacol* 2002; **79**: 81-87.

[13] Bhattacharya A, Chatterjee A, Ghosal S, Bhattacharya SK. Antioxidant activity of active tannoid principles of *Emblica officinalis* (amla). *Ind J Exp Biol* 1999; **37**: 676-680.

[14] Rege NN, Thatte UM, Dahanukar SA. Adaptogenic properties of six rasayana herbs used in Ayurvedic medicine. *Phytother Res* 1999; **13**: 275-291.

[15] Jeena KJ, Joy KL, Kuttan R. Effect of *Emblica officinalis*, *Phyllanthus amarus* and *Picrorrhiza kurroa* on *N*-nitrosodiethylamine induced hepatocarcinogenesis. *Can Lett* 1999; **136**: 11-16.

[16] Robak J, Gryglewski RJ. Flavonoids are scavengers of super oxide anions. *Biochem Pharmacol* 1988; **37**: 837-841.

[17] Husain SR, Cillard J, Cillard P. Hydroxyl radical scavenging activity of flavonoids. *Phytochem* 1987; **26**: 2489-2491.

[18] Lindeberg H, Krogdahl A. Laryngeal cancer and human papillomavirus: HPV is absent in the majority of laryngeal carcinomas. *Can Lett* 1999; **146**: 9-13.

[19] Rai M, Yadav A, Gade A. Silver nanoparticles as a new generation of antimicrobials. *Biotech Adv* 2009; **27**: 76-83.

[20] Hussain SM, Hess KL, Gearhart JM, Geiss KT, Schlager JJ. *In vitro* toxicity of nanoparticles in BRL 3A rat liver cells. *Toxicol Invitro* 2005; **19**: 975-983.

[21]Morones JR, Elechiguerra JL, Camacho A, Holt K, Kouri JB, Ramirez JT. The bactericidal effect of silver nanoparticles. *Nanotechnol* 2005; **16**: 2346

[22]Schrand AM, Braydich-Stolle LK, Schlager JJ, Dai L, Hussain SM. Can silver nanoparticles be useful as potential biological labels. *Nanotechnol* 2008; **19**: 235104.

[23]Braydich-Stolle L, Hussain SM, Schlager JJ, Hofmann MC. *In vitro* cytotoxicity of nanoparticles in mammalian germline stem cells. *Toxicol Sci* 2005; **88**: 412-419.

[24]Wang X, Yang L, Chen Z, Shin MD. Application of nanotechnology in cancer therapy and imaging. *Cancer J Clin* 2008; **58**: 97-110.

[25]Kim JS, Kuk E, Yu KN, Kim JH, Park SJ, Lee HJ, et al. Antimicrobial effects of silver nanoparticles. *Nanomed* 2007; **3**: 95-101.

[26]AshaRani PV, Mun GLK, Hande MP, Valiyaveettil S. Cyototoxicity and genotoxicity of silver nanoparticles in human cells. *ACS Nano* 2009; **3**: 279-290.

[27]Hwang IS, Lee J, Hwang JH, Kim KJ, Lee DG. Silver nanoparticles induce apoptotic cell death in *Candida albicans* through the increase of hydroxyl radicals. *FEBS J* 2012; **279**: 1327-1338.

[28]Roy N, Barik A. Green synthesis of silver nanoparticles from the unexploited weed resources. *Int J Nanotech App* 2010; **4**: 95-101.

[29]Mossman T. Rapid colorimetric assay for cellular growth and survival. *J Immunol Method* 1983; **65**: 55-63.

[30]Jesudason EP, Masilamani EG, Charles Jebaraj EJ, Solomon FD, Jayakumar RP. Efficacy of DL-a lipoic acid against systemic inflammation induced mice: antioxidant defense system. *Mol Cell Biochem* 2008; **313**: 113-123.

[31]Bhosle SM, Huilgol NG, Mishra KP. Enhancement of radiation-induced oxidative stress and cytotoxicity in tumor cells by ellagic acid. *Clin Chim Acta* 2005; **359**: 89-100.

[32]Lakshmi S, Dhanya GS, Joy B, Padmaja G, Remani P. Inhibitory effect of an extract of *Curcuma zedoaria* on human cervical carcinoma cells. *Med Chem* 2008; **17**: 335-334.

[33]Wyllie AH. Glucocorticoid-induced thymocyte apoptosis is associated with endogenous endonuclease activity. *Nature* 1980; **284**: 555-558.

[34]Niehaus WG, Samuelson B. Formation of melondialdehyde from phospholipids arachidonate during microsomal lipid peroxidation. *Eur J Biochem* 1986; **61**: 26-30.

[35]Kaakar ZYP, Das B, Visvanathan PN. A modified spectrophotometric assay of superoxide dismutase (SOD). *Ind J Biochem Biophy* 1984; **21**: 130-132.

[36]Sinha KA. Colorimetric assay of catalase. *Anal Biochem* 1972; **47**: 389-394.

[37]Rotruck JT, Pope A, Ganther HE. Selenium: biochemical roles as components of glutathione peroxidases. *Science* 1973; **179**: 588-590.

[38]Ellman GC. Tissue sulfydryl groups. *Arch Biochem Biophys* 1959; **32**: 70-77.

[39]Ahmad A, Mukherjee P, Senapati S, Mandal D, Khan MI, Kumar R, et al. Extracellular biosynthesis of silver nanoparticles using the fungus *Fusarium oxysporum*. *Coll Surf B Biointer* 2003; **28**: 313-318.

[40]Mirunalini S, Arulmozhi V, Shahira R. Diosgenin: a plant steroid induced apoptosis in human laryngeal carcinoma (Hep2) cells. *J Pharm Res* 2011; **4**: 2610-2614.

[41]Piao MJ, Kanga KA, Leeb IK, Kimb HS, Kimc S, Choid JY, et al. Silver nanoparticles induce oxidative cell damage in human liver cells through inhibition of reduced glutathione and induction of mitochondria-involved apoptosis. *Toxicol Lett* 2011; **201**: 92-100.

[42]Fadeel B, Ahlin A, Henter JI, Orrenius S, Hampton MB. Involvement of caspases in neutrophil apoptosis: regulation by reactive oxygen species. *Blood* 1998; **92**: 4808.

[43]Ott M, Gogvadze V, Orrenius S, Zhivotovsky B. Mitochondria, oxidative stress and cell death. *Apoptosis* 2007; **12**: 913-922.

[44]Ueda S, Masutani H, Nakamura H, Tanaka T, Ueno M, Yodoi J. Redox control of cell death. *Antioxid Redox Signal* 2002; **4**: 405-414.

[45]Hsin YH, Chen CF, Huang S, Shih TS, Lai PS, Chueh PJ. The apoptotic effect of nanosilver is mediated by a ROS and JNK dependent mechanism involving the mitochondrial pathway in NIH3T3 cells. *Toxicol Lett* 2008; **179**: 130-139.

[46]Green DR, Reed JC. Mitochondria and apoptosis. *Science* 1998; **281**: 1309-1312.

[47]Kroemer G, Zamzami N, Susin SA. Mitochondrial control of apoptosis. *Immunol Today* 1997; **18**: 44-51.

[48]Liu X, Kim CN, Yang J, Jemmerson R, Wang X. Induction of apoptotic program in cell-free extracts: requirement for dATP and cytochrome c. *Cell* 1996; **86**: 147-157.

[49]Li P, Nijhawan D, Budihardjo I, Srinivasula SM, Ahmad M, Alnemri ES, et al. Cytochrome c and dATP-dependent formation of Apaf-1/caspase-9 complex initiates an apoptotic protease cascade. *Cell* 1997; **91**: 479-489.

[50]Zou H, Henzel WJ, Liu X, Lutschg A, Wang X. Apaf-1, a human protein homologous to C. elegans CED-4, participates in cytochrome c dependent activation of caspase-3. *Cell* 1997; **90**: 405-413.

[51]Foldbjerg R, Olesen P, Hougaard M, Dang DA, Hoffmann HJ, Autrup H. PVP-coated silver nanoparticles and silver ions induce reactive oxygen species, apoptosis and necrosis in THP-1 monocytes. *Toxicol Lett* 2009; **190**: 156-162.

[52]Ponarulselvam S, Panneerselvam C, Murugan K, Aarthi N, Kalimuthu K, Thangamani S. Synthesis of silver nanoparticles using leaves of Catharanthus roseus Linn. G. Don and their antiplasmodial activities. *Asian Pac J Trop Biomed* 2012; **2**(7): 574-580.

[53]Mukunthan KS, Elumalai EK, Patel TN, Murty VR. Catharanthus roseus: a natural source for the synthesis of silver nanoparticles. *Asian Pac J Trop Biomed* 2011; 1(4): 270-274.

[54]Prasad TNVKV, Elumalai EK, Khateeja S. Evaluation of the antimicrobial efficacy of phytogenic silver nanoparticles. Asian Pac J Trop Biomed 2011; Supple 1(1): S82-S85.

[53]Park EJ, Yi J, Chung KH, Ryu DY, Choi J, Park K. Oxidative stress and apoptosis induced by titanium dioxide nanoparticles in cultured BEAS-2B cells. *Toxicol Lett* 2008; **180**: 222-229.

[54]Chen X, Deng C, Tang S, Zhang M. Mitochondria-dependent apoptosis induced by nanoscale hydroxyapatite in human gastric cancer SGC-7901 cells. *Biol Pharm Bull* 2007; **30**: 128-132.

[55]Oberdorster E. Manufactured nanomaterials (fullerenes C60) induce oxidative stress in brain of juvenile largemouth bass. *Environ Health Perspect* 2004; **112**: 1058-1062.

[56]Tirkey N, Pilkhwal S, Kuhad A, Chopra K. Hesperidin, a citrus bioflavonoid, decreases the oxidative stress produced by carbon tetrachloride in rat liver and kidney. *BMC Pharmacol* 2005; **5**: 2.

[57]Krishnaveni M, Mirunalini S. Therapeutic potential of *Phyllanthus emblica* (amla): the ayurvedic wonder. *J Bas Clin Physiol Pharmacol* 2010; **21**: 93-105.